Metallurgical and Materials Data 2, no. 2 (2024): 47-50

Publisher: Association of Metallurgical Engineers of Serbia

Metallurgical and Materials Data

www.metall-mater-data.com

Mechanical properties of mullite investigated by nanoindentation

Jovana Ružić[1]*, Jelena Maletaškić[1], Željko Radovanović[2], Svetlana Ilić[1]

[1] *Department of Materials, "Vinča" Institute of Nuclear Sciences – National Institute of the Republic of Serbia, University of Belgrade, PO Box 522, 11001 Belgrade, Serbia*
[2] *Innovation Center of the Faculty of Technology and Metallurgy, University of Belgrade, Karnegijeva 4, Belgrade, Serbia*

ARTICLE INFORMATION:

https://doi.org/10.56801/MMD29

Received: 30 May 2024
Accepted: 17 June 2024

Type of paper: Research paper

ABSTRACT

The mechanical behavior of sintered mullite material was studied using nanoindentation tests. Mullite compact was obtained by cold pressing sol-gel synthesized mullite precursor powder and sintering at 1550 °C. Analysis of the microstructural parameters and phase composition was done by XRD (X-ray diffraction) and SEM-EDS (scanning electron microscopy with energy dispersive X-ray spectrometry). A Berkovich indenter was employed for nanoindentation measurements at various loads (1000-9000 μN). After each test, in situ SPM (scanning probe microscopy) imaging was performed. The XRD pattern of sintered mullite displayed peaks of mullite (93.3%) and corundum (6.7%). Results revealed average values of hardness and elastic modulus of sintered mullite as 15.55 GPa and 174.37 GPa, respectively. Moreover, nanoindentation results indicated that mullite follows the Hall-Petch hardening relation due to the presence of grains with a size range of 0.2-2 μm. Indentation in areas with smaller grains exhibits higher hardness values. Post-test SPM images disclosed the presence of pile-ups around the indents, which were formed under loads higher than 3000 μN.

Keywords: mullite, mechanical properties, nanoindentation.

1. Introduction

Mullite is undoubtedly one of the most significant materials in traditional and advanced ceramics (Schneider, Fischer, and Schreuer 2015). Its exceptional properties like high melting point, low coefficient of thermal expansion, high chemical stability, and high creep resistance affirm it for many technological applications during the last decades. Besides its widespread traditional use in pottery, whiteware, porcelain, and refractories in the steel, cement, glass, and chemical industries, the advanced applications of mullite are also extensive covering the demanding fields and employing it as refractories, crucibles, optical materials, dental components, thermocouple tubes, heat exchangers, porous filters, hot gas filters, catalytic converter supports, and burner tubes (Schneider, Fischer, and Schreuer 2015; Aksay, Dabbs, and Sarikaya 1991; Krenzel et al. 2019; Biswal et al. 2021). However, the low thermal conductivity leads to poor sinterability, conducting to low fracture toughness, appointing mullite as a brittle material. It inherently limits the industrial applications of mullite ceramics. Meanwhile, sufficient hardness can be obtained by manufacturing using advanced consolidation methods, e.g., spark plasma sintering (SPS) (Ghahremani, Ebadzadeh, and Maghsodipour 2015; Ren et al. 2015; Rajaei et al. 2016) and high pressure sintering (Ilić et al. 2016). These advanced densification methods develop the unique grain morphology (elongated or needle-like), which has a property-controlling influence. So, the formed microstructural features, their size, distribution, and occurrence need to be carefully followed, controlled, and led to obtaining the material with improved mechanical properties. On the other hand, the powder synthesis procedure and the choice of suitable precursors can also influence the microstructure and, hence, the mechanical properties of mullite monoliths (Ebadzadeh 2003; Liu et al. 2020).

Nanoindentation testing is one of the well-established, non-destructive techniques for the mechanical characterization of bulk materials, coatings, and thin films at the nanoscale, which could be performed at room and elevated temperatures (Ruzic et al. 2019). Modern nanoindentation equipment can assemble and analyze large amounts of automatically collected data and later provide statistically evaluated results. This method is the most suitable for assessing the local mechanical properties of heterogeneous materials, composites, and biomaterials at the nanoscale (Luo et al. 2018; Li, Li, and Wang 2019; Nath et al. 2009; Karimzadeh et al. 2019). In cement-based materials, different nanomechanical techniques provide hardness and elastic modulus (plasticity), adhesion, bond strength, and nanotribological data of various phases in heterogeneous materials (Luo et al. 2018; Li, Li, and Wang 2019). Besides building materials, the nanoindentation probe of hydroxyapatite – mullite composites showed lower values of

* Corresponding author.
E-mail address: jruzic@vinca.rs (Jovana Ružić).

hardness and elastic modulus for composites (< 4GPa) than for pure materials, mullite (~9 GPa) and hydroxyapatite (~5 GPa) caused by the phase transformation and new phase formation at grain boundaries during thermal treatment leading to the deterioration of mechanical properties of the composites (Nath et al. 2009). The adjustment of nanoindentation testing obtains precise results and less error of global response compared to the macro-scale tests despite the asymmetric triangle in the spacemen-indenter contact area (Karimzadeh et al. 2019). Along the hardness and elastic modulus values, nanoindentation and nanostratch tests contribute to the adhesion strength data of thin mullite films. After nanostrach tests, any evidence of delamination on the coating/substrate interface did not appear, which leads to the conclusion that interfacial adhesion between coating and substrate (SiC) was reliable (Botero et al. 2011; 2012).

In this study, nanoindentation tests were employed to determine the mechanical behavior of sintered mullite material. Phase composition and microstructure were analyzed using XRD and SEM-EDS. The aim of this work is to expose the correlation between grain size and hardness of observed sintered mullite. Quantitative characterization of mullite deformation behavior was discussed based on post-test in situ SPM images.

2. Experimental work

Mullite precursor powder was prepared combining sol–gel and combustion methods, and heat treated at 800 °C for 4 hours. Detailed description of synthesis procedure is given in previous study (S. Ilić et al. 2014). Synthesized mullite powders were cold pressed under 400 MPa, and then sintered at 1550 °C for 4 hours in air. Samples height were 5 mm, with 8 mm in diameter.

Microstructure was investigated by MIRA3 TESCAN scanning electron microscope (SEM) with Energy Dispersive X-ray Spectrometry (EDS). Structural parameters and phase composition was analyzed using X-ray diffraction (XRD) carried out at Rigaku Ultima IV with Cu diffractometer, using D/teX Ultra detector and K-beta filter, at 40 kV, 40 mA. Scanning parameters were: step of 0.02 deg., scan range of 10°-90°, and 10 deg./min scan speed. PDXL2 software (PDXL version 2.0.3.0) was used for XRD pattern analysis with reference to the patterns of the International Centre for Diffraction Data database (ICDD), version 2012, where Williamson-Hall method was employed for crystallite size and lattice strain calculation. Nanoindentation measurements were performed using Hysitron TI950 Triboindenter, equipped with in situ Scanning Probe Microscopy (SPM) imaging system, and Berkovich indenter. The hardness and elastic modulus are calculated using Tribofrom load-displacement curve using Oliver–Pharr method (Oliver and Pharr 1992). The set of nine indents was done, with applied loads from 1000-9000 μN, loading rate 50 μN/s, and dwell time 10 s, with spacing between indents 15 μm, at room temperature. Post-test SPM imaging was used for quantitative characterization of mullite deformation behavior.

3. Results and discussion

The phase composition of sintered mullite is given of in Figure 1, where the XRD pattern indicates peaks of mullite (ICCD card no. 00-062-0481, formula: Al4.8Si1.2O9.6) and corundum (ICCD card no. 01-073-5928 formula: Al2O3). Quantitative analysis of this XRD pattern, done by PDXL software, showed that the content of the observed sample is 93.3% mullite and 6.7% corundum. The extracted structural parameters are given in Table 1 where crystallite size and lattice strain were calculated using the Williamson-Hall method. The results show that mullite possesses higher crystallite size and lower strain values compared to corundum.

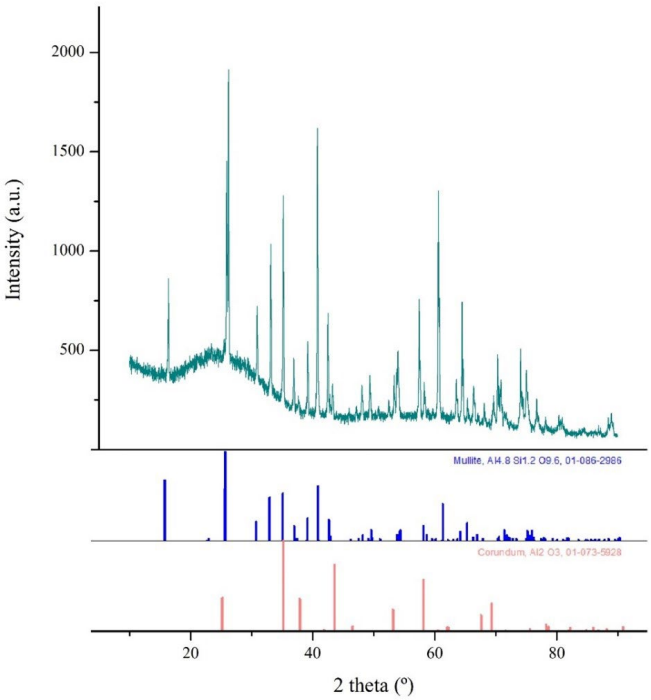

Fig. 1. XRD pattern of sintered mullite with identified phases mullite and corundum.

The microstructure of sintered mullite (Figure 2) was investigated using SEM-EDS. By observing the SEM micrograph, smaller and bigger grains appeared. Smaller equiaxed grains are around 0.5 μm in diameter, while the bigger elongated ones are around 1.5 μm in length. Smaller grains are abundant compared to bigger ones. Elemental analysis, performed by EDS, showed presence of the 48 wt.% O, 37.5 wt.% Al, 13.2 wt.% Si, which confirmed obtained XRD results.

Load-displacement curves of sintered mullite with corresponding SPM image are given in Fig.3. It can be noted that all load-displacement (LD) curves show similar slope of the loading part regarding the load increment. As it is expected, with increasing the load, the maximum depth (hmax) and contact depth (hc) of indents increase (Table 2, Figure 3). Formation of pile-ups around the indentation marks can be observed on SPM images (Figure 3), indicating dislocation movements under the indenter. The load of 1000 μN (Figure 3a) was used to investigate hardness on the grain boundary between two elongated grains. The test shows a very high hardness value, but the lowest value of elastic modulus compared to other tests. Nanoindentation measurements with applied loads of 2000, 3000, and 4000 μN (Figure 3 b, c, and d, respectively) are performed in small grain interior. These results expose that similar values of H and Er are obtained with applied loads of 2000 and 4000 μN, while values of H and Er calculated from the LC curve with an applied load of 3000 μN are significantly higher. The load of 5000 μN (Figure 3e) was applied on an area covering three small grans which exhibited the highest value of Er recorded of all measurements. Loads of 6000 and 7000 μN (Figure 3 f and g) were used for analysis of the mechanical properties of bigger grains. Further, loads of 8000 and 9000 μN (Figure 3 h and i) were applied to an area containing smaller and bigger grains. The average values of the hardness and elastic modulus of sintered mullite obtained from nanoindentation tests are 15.55±1.46 GPa, and 174.37 ± 10.42 GPa, respectively.

The results indicate that with increasing the applied load, values of hardness and elastic modulus are changing. The highest value of hardness was recorded with 9000 μN applied load, while the highest value of elastic modulus was after the applied load of 5000 μN (z). Higher values of hardness were achieved owing to Hall-Petch hardening, where the presence of small grains strongly contributes to hardness increase. In this research, the mullite sample showed a higher hardness value, determined by the nanoindentation technique, than

Table.1. Structural parameters of present phases in sintered mullite obtained from XRD pattern.

	Lattice parameter, [Å]			Cell volume, V(Å3)	Crystallite size, D [nm]	Lattice strain, ε [%]
	a	b	c			
Mullite	7.5568	7.6987	2.8865	167.93	36.1	0.15
Corundum	4.7660	4.7660	12.996	255.64	17.9	0.28

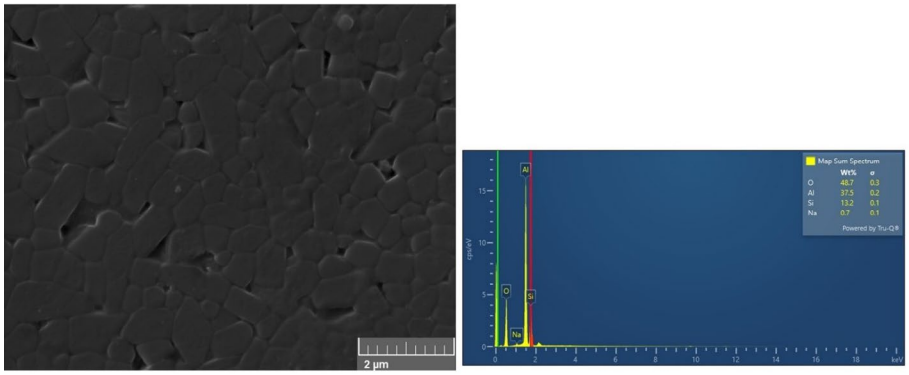

Fig.2. SEM micrographs of sintered mullite with EDS results.

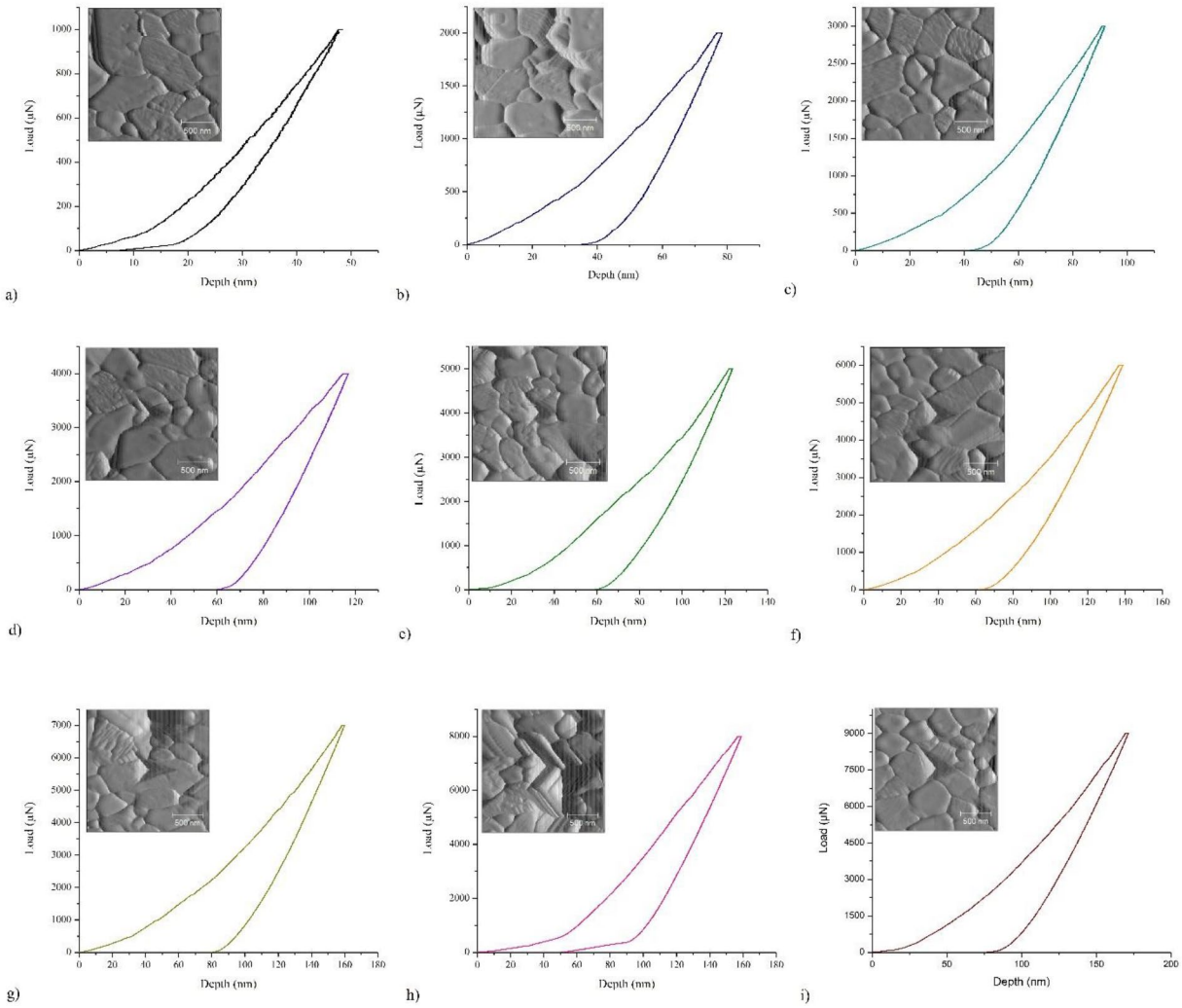

Fig. 3. Load-displacement curves at various applied load with corresponding SPM images of indents in sintered mullite surface: a) 1000 µN, b) 2000 µN, c) 3000 µN, d) 4000 µN, e) 5000 µN, f) 6000 µN, g) 7000 µN, h) 8000 µN, and i) 9000 µN.

previously published data (Nath et al. 2009). Even though the bulk density of sintered mullite at 1550 °C for 4 hours is not high enough to guarantee higher values of hardness (~79 %TD) (Svetlana Ilić et al. 2020), the produced samples exhibited more than satisfactory hardness values, which can be due to anisotropy, i.e., its unique crystal structure and microstructure. It recommends mullite to its potential application in the industry trying to overcome the essential problem of brittleness.

Table 2. Results of nanoindentation tests performed at various loads on sintered mullite.

Maximum load, Pmax (μN)	Contact depth, hc (nm)	Maximum depth, hmax (nm)	Final depth, hf (nm)	Young modulus, Er (GPa)	Hardness, H (GPa)
1000	31.81	48.42	16.64	162.86	15.50
2000	58.01	78.48	41.94	166.91	13.11
3000	66.31	92.03	48.43	180.97	16.04
4000	87.29	117.11	65.18	166.52	13.87
5000	92.84	123.71	57.33	192.76	15.70
6000	100.49	138.99	67.26	173.25	16.55
7000	118.85	160.09	83.88	164.82	14.62
8000	117.48	159.16	89.37	186.46	17.04
9000	123.75	171.67	87.11	174.80	17.56

4. Conclusions

In this work, the mechanical properties of sintered mullite were investigated using nanoindentation. Microstructural parameters were extracted from the XRD pattern, which confirmed that mullite is the dominant phase (93.3%) over corundum. Nanoindentation measurements show that with increasing the applied load maximum and contact depth increase. On the other hand, the values of hardness and elastic modulus change with applied load with respect to gran size involved. Dislocation movements were confirmed by pile-ups recorded around indentation marks using SPM imaging. The mullite sintered sample showed an outstanding hardness value with the potential for its improvement, i.e., by doping, and the potential use in industry, mainly in refractory.

It is known that nanoindentation is a very useful and powerful tool when local hardness at the nanoscale needs to be investigated. The present work demonstrates that grain size extremely influences the mechanical properties of sintered mullite. Moreover, by controlling the grain size the mullite could be considered a material with high dislocation density i.e. excellent hardness and elastic modulus which provides support for further research on this topic, and opens numerous application possibilities.

Acknowledgments

This work was funded by the Ministry of Education, Science and Technological Development of the Republic of Serbia, Contract No. 451-03-66/2024-03/200017, and 451-03-66/2024-03/200287.

References

Aksay, Ilhan A., Daniel M. Dabbs, and Mehmet Sarikaya. “Mullite for structural, electronic, and optical applications.” Journal of the American Ceramic Society 74, no. 10 (1991): 2343-2358.

Biswal, Bijaylaxmi, D.K. Mishra, Satyaprakash Narayan Das, and Satyanarayan Bhuyan. “Structural, micro-structural, optical and dielectric behavior of mullite ceramics.” Ceramics International 47, no. 22 (2021): 32252-32263.

Botero, C.A., E. Jimenez-Piqué, T. Kulkarni, G. Fargas, V.K. Sarin, and L. Llanes. “Cross-sectional nanoindentation and nanoscratch of compositionally graded mullite films.” Surface and Coatings Technology 206, no. 7 (2011): 1927-1931.

Botero, C.A., E. Jimenez-Piqué, J. Seuba, T. Kulkarni, V.K. Sarin, and L. Llanes. “Mechanical behavior of 3Al2O3·2SiO2 films under nanoindentation.” Acta Materialia 60, no. 16 (2012): 5889-5899.

Ebadzadeh, T. “Formation of mullite from precursor powders: Sintering, microstructure and mechanical properties.” Materials Science and Engineering: A 355, no. 1-2 (2003): 56-61.

Ghahremani, D., T. Ebadzadeh, and A. Maghsodipour. “Spark plasma sintering of mullite: Relation between microstructure, properties and spark plasma sintering (SPS) parameters.” Ceramics International 41, no. 5 (2015): 6409-6416.

Ilić, S., S. Zec, M. Miljković, D. Poleti, M. Pošarac-Marković, Dj. Janaćković, and B. Matović. “Sol–gel synthesis and characterization of iron doped mullite.” Journal of Alloys and Compounds 612 (2014): 259-264.

Ilić, Svetlana, Valentin N. Ivanovski, Željko Radovanović, Adela Egelja, Maja Kokunešoski, Aleksandra Šaponjić, and Branko Matović. “Structural, microstructural and mechanical properties of sintered iron-doped mullite.” Materials Science and Engineering: B 256 (2020): 114543.

Karimzadeh, A., S. S. R. Koloor, M. R. Ayatollahi, A. R. Bushroa, and M. Y. Yahya. “Assessment of nano-indentation method in mechanical characterization of heterogeneous nanocomposite materials using experimental and computational approaches.” Scientific Reports 9, no. 1 (2019): 15763.

Krenzel, Thomas F., Jürgen Schreuer, Derek Laubner, Michel Cichocki, and Hartmut Schneider. “Thermo-mechanical properties of mullite ceramics: New data.” Journal of the American Ceramic Society 102, no. 1 (2019): 416-426.

Li, Yaqiang, Yue Li, and Rui Wang. “Quantitative evaluation of elastic modulus of concrete with nanoidentation and homogenization method.” Construction and Building Materials 212 (2019): 295-303.

Liu, Dazhao, Kaixuan Gui, Jianzhou Long, Yu Zhao, Wenbo Han, and Gang Wang. “Low-temperature densification and mechanical properties of monolithic mullite ceramic.” Ceramics International 46, no. 8 (2020): 12329-12334.

Luo, Zhiyu, Wengui Li, Kejin Wang, and Surendra P. Shah. “Research progress in advanced nanomechanical characterization of cement-based materials.” Cement and Concrete Composites 94 (2018): 277-295.

Nath, Shekhar, A. Dey, A.K. Mukhopadhyay, and Bikramjit Basu. “Nanoindentation response of novel hydroxyapatite–mullite composites.” Materials Science and Engineering: A 513-514 (2009): 197-201.

Oliver, W. C., and G. M. Pharr. “An improved technique for determining hardness and elastic modulus using load and displacement sensing indentation experiments.” Journal of Materials Research 7, no. 6 (1992): 1564-1583.

PDXL Version 2.0.3.0 Integrated X-ray Powder Diffraction Software. Tokyo, Japan: Rigaku Corporation, 2011.

Rajaei, Hosein, Iman Mobasherpour, Mohammad Farvizi, and Mohammad Zakeri. “Effect of mullite synthesis methods on the spark plasma sintering behaviour and mechanical properties.” Micro & Nano Letters 11, no. 8 (2016): 465-468.

Ren, Lin, Zhengyi Fu, Yucheng Wang, Fan Zhang, Jinyong Zhang, Weimin Wang, and Hao Wang. “Fabrication of transparent mullite ceramic by spark plasma sintering from powders synthesized via sol–gel process combined with pulse current heating.” Materials & Design 83 (2015): 753-759.

Ruzic, Jovana, Ikumu Watanabe, Kenta Goto, and Takahito Ohmura. “Nano-indentation measurement for heat resistant alloys at elevated temperatures in inert atmosphere.” Materials Transactions 60, no. 8 (2019): 1411-1415.

Schneider, Hartmut, Reinhard X. Fischer, and Jürgen Schreuer. “Mullite: Crystal structure and related properties.” Edited by D. J. Green. Journal of the American Ceramic Society 98, no. 10 (2015): 2948-2967.